Traffic of pairs of drops in microfluidic ladder networks with fore-aft structural asymmetry

Jeevan Maddala, William S. Wang, Siva A. Vanapalli & Raghunathan Rengaswamy

Microfluidics and Nanofluidics

ISSN 1613-4982
Volume 14
Combined 1-2

Microfluid Nanofluid (2013) 14:337-344
DOI 10.1007/s10404-012-1054-z

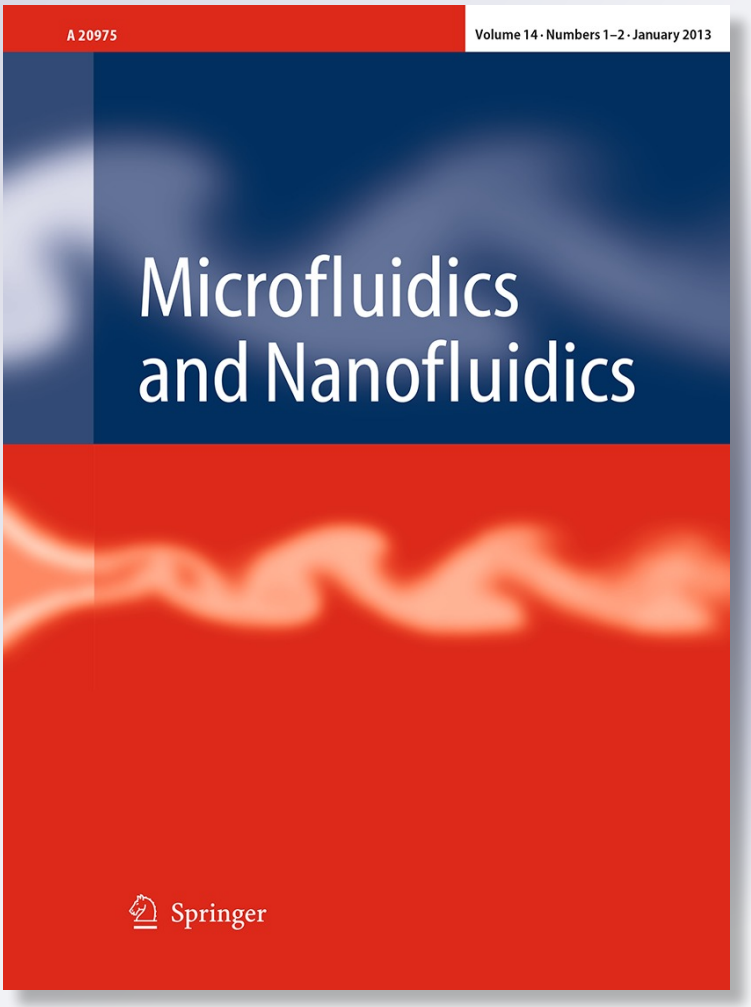

Springer

Your article is protected by copyright and all rights are held exclusively by Springer-Verlag. This e-offprint is for personal use only and shall not be self-archived in electronic repositories. If you wish to self-archive your work, please use the accepted author's version for posting to your own website or your institution's repository. You may further deposit the accepted author's version on a funder's repository at a funder's request, provided it is not made publicly available until 12 months after publication.

Springer

Author's personal copy

Microfluid Nanofluid (2013) 14:337–344
DOI 10.1007/s10404-012-1054-z

RESEARCH PAPER

Traffic of pairs of drops in microfluidic ladder networks with fore-aft structural asymmetry

Jeevan Maddala · William S. Wang · Siva A. Vanapalli · Raghunathan Rengaswamy

Received: 1 April 2012 / Accepted: 28 May 2012 / Published online: 23 October 2012
© Springer-Verlag 2012

Abstract We investigate the dynamics of pairs of drops in microfluidic ladder networks with slanted bypasses, which break the fore-aft structural symmetry of the network. Our analytical results indicate that unlike symmetric ladder networks, structural asymmetry introduced by a single slanted bypass can be used to modulate the relative drop spacing, enabling them to contract, synchronize, expand, or even flip at the ladder exit. Our experiments confirm all these behaviors predicted by theory. Numerical analysis further shows that while ladder networks containing several identical bypasses are limited to nearly linear transformation of input delay between drops, combination of forward and backward slanted bypasses can cause significant nonlinear transformation enabling coding and decoding of input delays.

Keywords Droplet spacing · Microfluidic networks · Non-linear dynamics · Passive control

1 Introduction

Understanding the spatiotemporal dynamics of confined droplets in interconnected fluidic paths is essential for applications in lab-on-chip technologies (Theberge et al. 2010; Song et al. 2006). The traffic of drops or bubbles in even simple networks such as bifurcating channels can be astonishingly complex due to collective hydrodynamic resistive interactions in the branches (Sessoms et al. 2010; Engl et al. 2005; Fuerstman et al. 2007). Although such intricate dynamics—in the case of lab-on-chip applications—make device design challenging, the passive collective behaviors can be harnessed to perform useful tasks such as droplet sorting (Cristobal et al. 2006) and storage (Bithi and Vanapalli 2010; Abbyad et al. 2011).

Recently, the collective dynamics between pairs as well as trains of drops have been harnessed in the so-called microfluidic ladder networks (MLNs) to control their relative drop spacing passively (Prakash and Gershenfeld 2007; Prakash et al. 2007; Hong et al. 2010; Ahn et al. 2011). In MLNs, two droplet-carrying parallel channels are connected by narrow bypass channels through which the motion of drops is forbidden but the carrier fluid can leak. Hong et al. (2010) showed that a vertical bypass added to parallel channels enhanced high-throughput synchronization of drops and their coalescence downstream of the network. Ahn et al. (2011) used ladder networks to synchronize trains of droplets and showed that complex pairing of drops can occur depending on droplet size, production frequency and flow rates. Lee et al. (2011) demonstrated combinatorial pairing of drops, using two interconnected ladder networks, with droplet transport occurring only in one of the parallel channels of the ladders.

Current experimental designs (Prakash and Gershenfeld 2007; Prakash et al. 2007; Hong et al. 2011; Ahn et al. 2011) of ladders have fore-aft structural symmetry due to equally spaced vertical bypasses. Moreover, in all cases the droplets are driven by a constant flow rate at the inlet of the ladder and are exposed to constant pressure at the outlet. Recent work (Schindler and Ajdari 2008) has shown that in symmetric ladders, the distance between the pairs of drops

J. Maddala · W. S. Wang · S. A. Vanapalli (✉) · R. Rengaswamy (✉)
Department of Chemical Engineering,
Texas Tech University, Lubbock, TX 79401-3121, USA
e-mail: siva.vanapalli@ttu.edu

R. Rengaswamy
e-mail: raghu.rengasamy@ttu.edu

Author's personal copy

can only decrease at the exit for constant inlet flow rate and constant pressure at the exit. Alternatively, by changing the flow boundary conditions to constant pressure at the inlet, and constant flow rate at the outlet, the relative separation between droplet pairs can be made to increase. Since flexible manipulation of drop spacing in networks is crucial for passively regulating a variety of tasks including drop coalescence (Hong et al. 2010), detection (Baret et al. 2009) and storage (Bithi and Vanapalli 2010; Abbyad et al. 2011), there is a need to design microfluidic ladders that allow facile control of drop spacing, regardless of the boundary conditions at the entrance and exit of the ladder.

From a fundamental perspective, the dynamics of drops in MLNs is distinct compared to the widely studied microfluidic loops (Sessoms et al. 2010; Schindler and Ajdari 2008; Fuerstman et al. 2007; Belloul et al. 2009). In loops, drops at junctions choose the branch with the highest flow rate. These discrete choices make such systems non-linear, enabling coding and decoding of input signals (Fuerstman et al. 2007). Since drops do not typically make decisions at the bypass junctions in ladders, an open question is whether it is possible to design microfluidic ladders that yield significant non-linear transformation of input signal (i.e., inter-droplet spacing at the ladder entrance).

In this article, we study the dynamics of spacing between drop pairs in MLNs with slanted bypasses. We find that because the slant breaks the fore-aft symmetry, for the commonly used boundary condition of constant flow rate at the inlet and constant pressure at the ladder outlet, it provides significantly more control over drop spacing than symmetric MLNs. We also discover that inclusion of slanted bypasses in ladders can non-linearly transform the initial delay between drops. These advanced capabilities arise because slanted bypasses flexibly manipulate (1) the locations in the channels where drop velocity changes occur and (2) the time drops spend with bypasses between them.

2 Basic description of drop spacing in MLNs

In our work, we consider only droplet pairs, i.e., a droplet pair leaves the ladder before the next one is introduced. As shown in Fig. 1, the key framework for quantifying drop spacing in this case comes from understanding the variation in relative velocity (u) between drops in the top and bottom channel as they cross nodes in the network. Consider the simple case of a symmetric MLN with one vertical bypass. As shown in Fig. 1b left, when two drops driven by a constant flow rate (Q) enter the ladder with an initial separation (Δx_{in}), they maintain the same separation as $u = 0$. When the leading drop crosses the node, a new configuration (see Fig. 1b center) is reached, and the relative velocity changes as fluid leaks into the bypass, i.e., $u < 0$, causing a contraction in inter-drop distance. When both drops cross the bypass, $u = 0$ again as the pressure drop across the bypass is zero due to equal downstream branch resistances (see Fig. 1b right). Thus, the outlet drop spacing, (Δx_{out}), is less than the initial separation and is given by $\Delta x_{\text{out}} = \Delta x_{\text{in}} + u\Delta T$, where ΔT is the duration the drops remain in the particular configuration of Fig. 1b center.

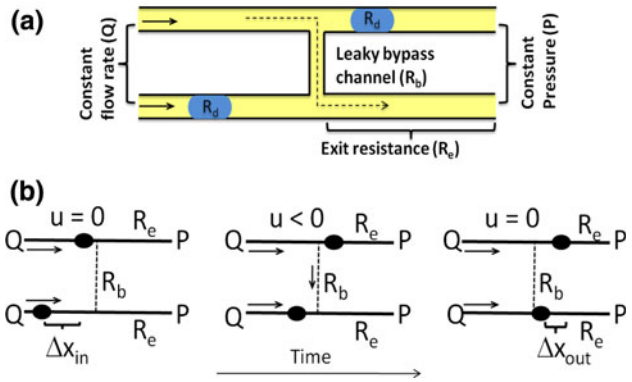

Fig. 1 **a** Ladder with a *vertical* bypass with a constant flowrate (Q) at inlets and constant pressure (P) at outlet channels. **b** Three distinct configurations are possible when a pair of drops traverses through a *symmetric* ladder network. *Black objects* represent drops. R_d, R_b and R_e denote the hydrodynamic resistance of drop, bypass and exit channel respectively, and u denotes the relative velocity between the pair of droplets. *Full* and *dashed lines* denote transport and bypass channels respectively. *Arrows* show flow direction

In networks with many bypasses, more drop configurations and relative velocity changes are possible than that in Fig. 1b as drops traverse through multiple nodes. In general, we find that

$$\Delta x_{\text{out}} = \Delta x_{\text{in}} + \sum_{j=1}^{p} u_j \Delta T_j \tag{1}$$

where p is the number of distinct configurations of droplets occurring in the network, u_j and ΔT_j are the associated relative velocities and time periods.

The degree of separation achieved at the ladder exit depends on the contribution of the summation term in Eq. (1), both with respect to magnitude and sign. The strength of this contribution is modulated by the specific architecture of the ladder network. To compute this contribution, we use resistive network modeling (Schindler and Ajdari 2008; Maddala et al. 2012), where we assume each drop is a point object with the same hydrodynamic resistance (R_d). Since the drop velocity (V) is linearly dependent on liquid flow rate (Q), we have $V = \beta Q/S$, where S is the channel cross-sectional area and β is the slip factor, $0 < \beta < 2$ (Jakiela et al. 2011). To preserve the relative separation when drops leave the ladder network, we choose the downstream channel resistances to be equal.

Author's personal copy

3 Effect of single interconnected bypass

We begin by discussing the effect of a single slanted bypass in regulating the dynamics of drop spacing. Figure 2a, b shows a representative ladder network with a slanted bypass. In contrast to the vertical bypass, a new control parameter, ΔL, is needed to describe two possible structural configurations—backward slant for $\Delta L < 0$ and forward slant for $\Delta L > 0$. The definitions of forward and backward slants are based on first identifying the leading droplet and choosing the viewing perspective that enables $\Delta x_{\text{in}} \geq 0$; therefore in our study, the sign of Δx_{in} is assumed to be positive, and the sign of ΔL varies. This analysis will be the same as having the sign of ΔL fixed and allowing the sign of Δx_{in} to vary.

To determine the drop spacing at the exit due to the slanted bypass, we identify the relative velocities that are non-zero and the corresponding durations as prescribed by Eq. (1). Similar to the vertical bypass in Fig. 1, non-zero u occurs only after one of the droplets crosses a node. Assuming that the leading droplet crosses the node first, the relative velocity (u) is $-\beta Q_{\text{b}}/S$, where Q_{b} is the flow in bypass. Solving the hydrodynamic circuit for this drop configuration analytically, we obtain $Q_{\text{b}} = Q\ R_{\text{d}}/(R_{\text{b}} + 2R_{\text{e}} + R_{\text{d}})$. Therefore, $u = -\beta Q/S \cdot (R_{\text{d}}/(R_{\text{b}} + 2R_{\text{e}} + R_{\text{d}}))$ and $\Delta T = (\Delta x_{\text{in}} - \Delta L)S/(\beta Q)$, where R_{b} and R_{e} are the bypass and exit channel resistances, respectively. Thus, Eq. (1) for the case of an MLN with a slanted bypass transforms to

$$\Delta x_{\text{out}} = \Delta x_{\text{in}} - M(\Delta x_{\text{in}} - \Delta L) \tag{2}$$

where $M = R_{\text{d}}/(R_{\text{b}} + 2R_{\text{e}} + R_{\text{d}})$ and $0 < \text{M} < 1$. Note in Eq. (2), $\Delta x_{\text{in}} > 0$ corresponds to the top drop leading over the bottom drop in the ladder.

Remarkably, Eq. (2) captures several dynamical regimes emerging from structural asymmetry due to a slanted bypass as illustrated in Fig. 2c. For the particular case of a vertical bypass ($\Delta L = 0$), Eq. (2) reveals that drops can only undergo contraction (see Fig. 1a). Moreover, perfect synchronization of drop pairs, i.e., $\Delta x_{\text{out}} = 0$, is difficult to achieve with a single vertical bypass, as it requires M to be unity.

In contrast to the vertical bypass, we find that the backward slant, where $\Delta L < 0$, yields flexible control over drop spacing as illustrated in Fig. 2c. For large input drop spacing, $\Delta x_{\text{in}} > \frac{M\Delta L}{M-1}$ the pairs at the exit undergo contraction for the same reason as in the vertical bypass. Perfect synchronization can also be realized with just a single backward slant when $\Delta x_{\text{in}} = \frac{M\Delta L}{M-1}$. Moreover, when $\Delta x_{\text{in}} < \frac{M\Delta L}{M-1}$, a new regime emerges that we refer to as *flipping*. We observe that the leading droplet is initially ahead of the lagging droplet. However, when the leading drop crosses the bypass first, its velocity is reduced and the lagging drop has sufficient duration to catch up and overtake it. Thus, the flipping behavior yields $\Delta x_{\text{out}} < 0$ as shown in Fig. 2c.

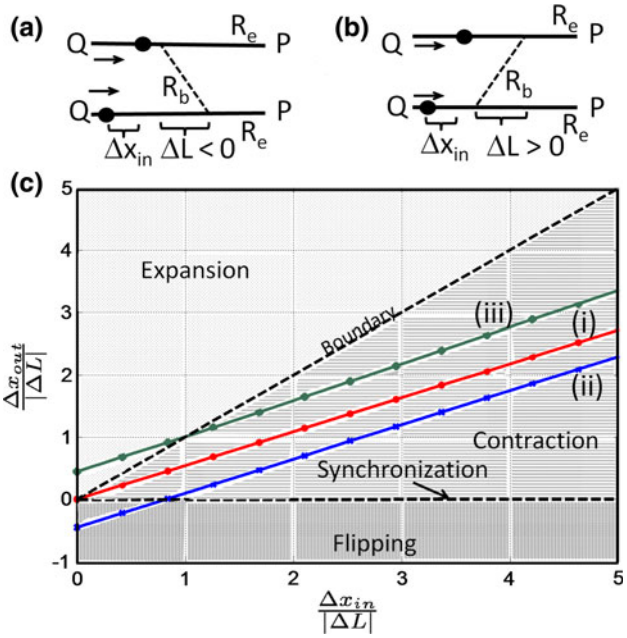

Fig. 2 Ladder networks with **a** backward slant and **b** forward slant; **c** dynamical regimes due to drop traffic in MLNs with a single (*i*) vertical bypass (*ii*), backward slant and (*iii*) forward slant. $M = 0.45$

Similar to the backward slant, the forward slant (where $\Delta L > 0$) provides additional means of control. Interestingly, in contrast to the backward slant, the behavioral transitions depend only on the value of input drop spacing relative to ΔL. When $\Delta x_{\text{in}} < \Delta L$, the lagging drop crosses the bypass first, resulting in expansion as highlighted in Fig. 2c. Alternatively, if $\Delta x_{\text{in}} > \Delta L$, the leading droplet crosses the bypass first, resulting in contraction. If $\Delta x_{\text{in}} = \Delta L$, then both drops cross the bypass simultaneously and the input spacing is preserved. Thus, forward slant allows drop pairs to expand, contract or remain unchanged.

The above analysis is particularly valuable when designing optimal microfluidic structures based on functionality. Consider the following question: what would be the ideal microfluidic ladder device to synchronize pairs of droplets with a fixed inlet spacing d? Using the above theoretical analysis, a backward slanted bypass with a slant base of $\frac{d(1-M)}{M}$ is an optimal structure. Therefore, the analytical expressions given here help in designing single bypass ladder networks.

To obtain a succinct analytical expression between inlet and outlet drop spacing, the exit channels were assumed to have equal resistances, else the droplet spacing changes as the drops move along the length of the ladder network.

Author's personal copy

However, the predictions demonstrated in Fig. 2 are qualitatively valid for ladder networks with distinct exit branch resistances.

4 Materials and methods

We fabricated MLNs with a single slanted bypass in poly(dimethyl) siloxane (PDMS) using standard soft lithography techniques (Duffy et al. 1998). Figure 3 is a superposition of three experimental images showing a ladder network with a single backward slant and droplets at various positions. All devices had uniform channel heights of 100 μm and main upper and lower channel widths of 100 μm. The devices all share the same unique slant-base bypass geometry with an effective slant base (ΔL) of 500 μm, as seen in Fig. 3. Each slanted bypass connects to the upper and lower channels via narrow perpendicular connecting sections 50-μm wide by 100-μm long, where the lower connecting section is staggered 500-μm downstream of the upper connecting section. In Fig. 3, the top drop is in the midst of passing over the upper connecting section, while the lower drop has just passed the lower connecting section. The upper and lower connecting sections are joined by a larger mid-section that is 200-μm wide by 550-μm long and runs longitudinally, parallel to the upper and lower channels. Downstream of the bypass-connecting sections are upper and lower exit channels that combine into a single, 200-μm-wide central exit channel.

The hydraulic resistances of the upper and lower exit channels should be identical if one desires to preserve the contraction or expansion effect of the bypass at the end of the network. The easiest way to achieve this is to have upper and lower exit channels with identical lengths and cross sections. Our experimental devices therefore have staggered, equal-length exit segments that combine into a single exit channel, as seen in Fig. 3. To minimize the upper and lower exit segment resistances, we limited the upper and lower exit channel lengths to 1000 μm before co-terminating those channels and allowing their pressures to equalize. These staggered exit channels are joined by another chamber that is essentially the same shape as the bypass except for the addition of a larger channel leading up and away from the center of the longitudinal mid-section.

We estimate the resistances of the bypass and exit channel segments to be 0.97 kg/(mm^{4}s) and 0.85 kg/(mm^{4}s), respectively, using the analytical expression for hydraulic resistance due to Poiseuille flow of hexadecane through rectangular channels (Bruus 2008):

$$R = \frac{12\mu L}{h^3 w}\left[1 - \sum_{n,\,odd}^{\infty} \frac{1}{n^5}\frac{192}{\pi^5}\frac{h}{w}\tanh(n\pi w/2h)\right]^{-1} \quad (3)$$

where h, w and L are the height, width and length of the branch, respectively. The symbol μ represents the viscosity of the hexadecane oil, and n is the series index which takes only odd values. To estimate the resistance of the bypass, we take its value to be the sum of its three major segment resistances: the upper connecting segment, the mid-section and the lower connecting segment. Note that the bypass and exit channel resistances should be minimized as much as possible so that they are of the same order of magnitude or less compared to the droplet resistance. This guideline helps ensure a measurable contraction or expansion effect when one droplet passes the bypass before the other.

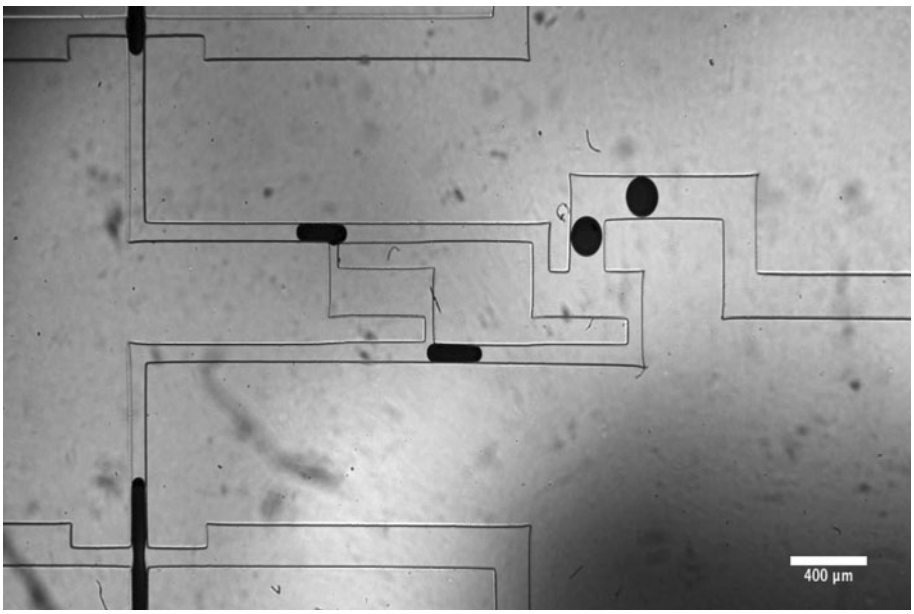

Fig. 3 Overlay of three superimposed images taken at different time points in an MLN with a single backward slant bypass. The three images correspond to: (1) droplet being produced at cross junctions, (2) droplets traveling along upper and lower main channels, and (3) droplets exiting. Aqueous droplets with 5 % v/v black dye in *hexadecane*. The overall flow rate is 202 μL/h with a 100:1 ratio of oil to aqueous flow rates

Author's personal copy

Pairs of dyed aqueous droplets (5 % by volume Higgins Black Calligraphy Ink, Chartpak Inc., Leeds, MA) in hexadecane were produced using identical cross-flow junctions in the upstream sections of the upper and lower channels (see Fig. 3). No surfactant was added into the continuous phase. Syringe pumps (PHD 2000, Harvard Apparatus, MA) delivered constant volumetric flow rates of 200 μL/h hexadecane and 2.0 μL/h dyed deionized (DI) water (no surfactant) into each parallel side of the device. To study the droplet motion, we took high-speed images using an inverted microscope (IX70, Olympus, PA) and a high-speed camera (Phantom V310, Vision Research, NJ) at 100 frames/s. We then used ImageJ software to manually measure droplet spacing in the longitudinal direction and to monitor its evolution over time.

5 Experimental analysis

To confirm the different behaviors predicted by our theory, we constructed an MLN with a single slant. It is important to note that the parameter space for designing MLNs is large, requiring optimization of upstream and downstream transport channel resistance, slant resistance, slant slope and hydrodynamic resistance of drops, which itself is a complex function of the flow conditions and fluid properties (Vanapalli et al. 2009; Labrot et al. 2009). Fortunately, insights from Eq. (2) reduce the search space. According to Fig. 2, the backward slant is the best candidate to achieve maximum contraction, perfect synchronization and flipping. Moreover, Eq. (2) reveals that if $\Delta x_{in} < 0$ (i.e., the top drop is lagging behind the bottom drop in the ladder), then the forward slant becomes a backward slant, allowing access to the expansion regime as well as the condition where the input separation does not change. Thus, we chose the backward slant to test our predictions.

We incorporated two cross-flow drop generators in polydimethyl(siloxane) devices to introduce drops at a constant flow rate into the ladder (see Sect. 4 for details on methods). To amplify the effects produced by the backward slant, we maximized the value of M by minimizing R_b and R_e. For example, as shown in Fig. 4a, the bypass has an enlarged mid-section to minimize R_b. We also ensured R_b and R_e to be $\sim O(R_d)$. In Fig. 4b, we show experimental curves corresponding to each of the dynamical regimes predicted by our theory. We find the drop spacing to be relatively unchanged when the drop pair is before or after the bypass. However, as pairs of drops cross the bypass section, their spacing may expand, contract, flip, synchronize or remain unchanged depending on the initial separation. By comparing the data of Fig. 4 with the expression for u (c.f. Sect. 3), we estimate $R_d \approx 1.2$ kg/mm^{4}s, $M \approx 0.2$ and $\beta \approx 0.82$. Droplet resistance was estimated

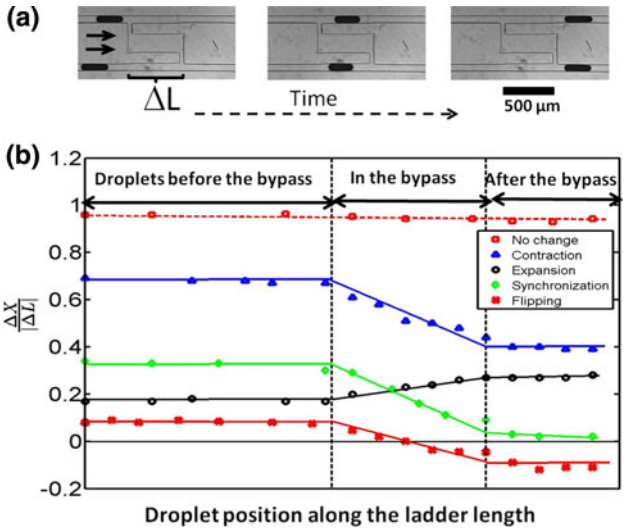

Fig. 4 Experimental confirmation of the dynamic behaviors in MLNs: **a** *snapshots* showing synchronization of a droplet pair. Time interval between images is 0.08 s; **b** drop spacing as a function of position in the ladder ($|\Delta L| = 500$ μm. Hexadecane was in continuous phase, and aqueous dye solution was in dispersed phase. The transport channels are 100-μm wide and tall

by solving for R_d in the expression for relative velocity u after substituting the values for all other parameters, which were either measured (u, β, Q, S) or estimated from existing analytical expressions (R_b, R_e). Taken together, our analytical results and experiments suggest that MLNs with slanted bypasses provide greater flexibility in controlling droplet spacing than ladders with vertical bypasses.

6 Effect of multiple bypasses

To understand the flexibility due to additional bypasses, we investigated ladders containing several identical bypasses. In contrast to the single bypass case, in ladders with n bypasses, the maximum number of configurations where u is non-zero is $n(n + 1)/2$. However, all these configurations need not be realized for a given Δx_{in}, which makes the theoretical analysis complex. We therefore used resistive network-based simulations (Schindler and Ajdari 2008) to fully quantify the exit drop spacing for arbitrary input delay. As shown in Fig. 5a, we find that additional vertical bypasses simply amplify the contraction effect due to a single bypass, i.e., slope decreases with increasing number of bypasses. A similar outcome also holds, as shown in Fig. 5b, for the particular case of an MLN with forward slants. We also find that the largest change in drop spacing occurs in the first few bypasses. Ladders with multi-bypasses could therefore be useful to maintain the same behavior as their single bypass counterparts, while dampening the effect of small fluctuations in input drop

Author's personal copy

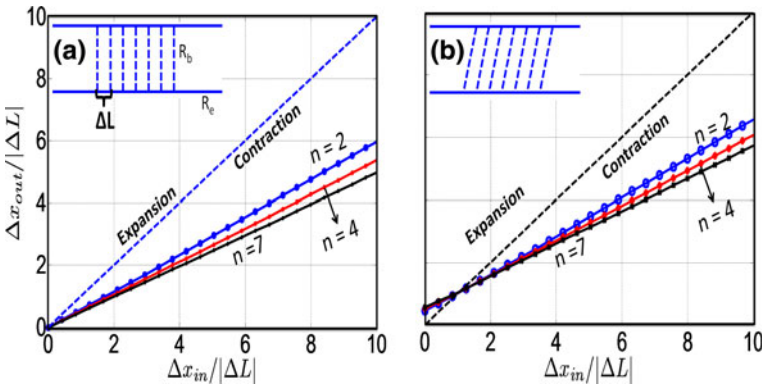

Fig. 5 Ladder networks with multiple identical bypasses: **a** vertical bypasses, **b** forward slants, $R_d/R_b = 3, R_d/R_{\Delta L} = 22, R_d/R_e = 2, R_d = 1.5\,\mathrm{kg/mm^4 s}$ and $\beta = 1.4$

spacing. It is interesting to note that in vertical bypass ladders, as the number of bypasses(n) tend to infinity, $(\Delta x_{\mathrm{out}} \to 0)$, implying that they synchronize the drops. In contrast, for slanted networks, as $n \to \infty, (\Delta x_{\mathrm{out}} \to \Delta L)$, implying drop spacing asymptotically approach the geometry or the inter-bypass spacing of the ladder networks. Slanted networks thus show duality, both contraction and expansion of inlet spacing, whereas vertical bypasses only reduce inlet spacing.

Our analysis of MLN designs with identical bypasses has shown that at small input delay, drop spacing may either contract or expand, while it always contracts at large input delay (c.f. Fig. 5). The contraction at large input delay is expected because the leading drop is the first to cross the bypass and slow down. Initially, it appears that expansion is not possible at large input delays. To further probe this notion, we developed an evolutionary algorithm (Maddala and Rengaswamy 2012) to search for ladder designs containing any combination of slant and/or vertical bypasses that might be capable of contraction at low input spacing and expansion at large input spacing. Our search strategy revealed that such networks do exist, and an example is shown in Fig. 6a. The dynamics of drop spacing in this network cannot be rationalized from mere addition of functionalities of the single bypasses shown in Fig. 5. Instead, we find that the first five bypasses collectively cause contraction of drop spacing, while the last two bypasses cause drops to expand. However, the relative magnitudes of contraction and expansion from these sets of bypasses depend on the input drop spacing. We observe that at small input delays, the first five bypasses dominate resulting in contraction behavior (see Fig. 6a), whereas at large input delays, the last two bypasses dominate yielding expansion.

A striking observation from Fig. 6a is that the curve is significantly nonlinear compared to the almost linear dependence observed in ladders with identical bypasses. This result is significant because it implies nonlinear transformation of input delay without any droplet decision-making at bypass junctions. A unique consequence of this

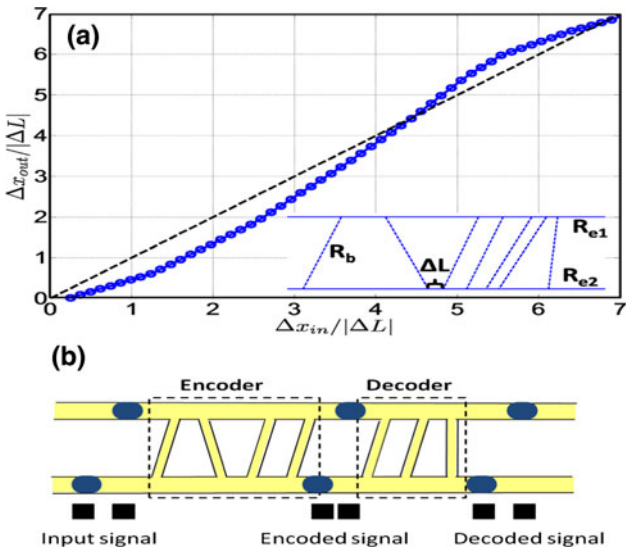

Fig. 6 **a** Nonlinear output delay in a ladder network containing a mixed combination of *slanted* and *vertical* bypasses (structure of the network is shown in *inset*). **b** Encoding and decoding signal using ladder network $R_d/R_b = 3R_d/R_{\Delta L} = 2.6, R_{e2}/R_{e1}$ is 1.01, $R_{e1}/R_d = 20$. $R_d = 1.5\,\mathrm{kg/mm^4 s}$ and $\beta = 1.4$

nonlinear transformation is the capability to encode and decode input delays as shown in Fig. 6b where the entrance delay between pairs of drops represents the input signal, and the system of bypasses represents the encoder and decoder. First, consider the curves in Fig. 4 where the input signal is 'scrambled' in the bypass section, but does not revert to its original value and therefore it is not decoded. In striking contrast, we find in Fig. 6a that the input signal gets encoded and decoded at two different values of $\frac{\Delta x_{\mathrm{in}}}{\Delta L} = 4.5, 7$ where $\Delta x_{\mathrm{in}} = \Delta x_{\mathrm{out}}$. At these input delays, we find that the above-discussed contraction and expansion effects introduced by sets of bypasses negate each other.

It is useful to consider the differences in codec characteristics of our ladder networks with those based on loops. We quantify the codec characteristics by measuring the relative change in magnitudes of encoded and decoded signals $(\frac{|\Delta x_f - \Delta x_{\mathrm{in}}|}{\Delta x_{\mathrm{in}}})$. In Fig. 6b, the input signal changes by

Author's personal copy

75.1 % as it gets encoded, and the decoded signal differs from input signal by 0.01 %, whereas in loop systems, the encoded signal and decoded signals differ from the input signal by an average of 33.3 and 2.3 %, respectively (Fuerstman et al. 2007). The encoder/decoder illustration of Fig. 6 is just an exemplary demonstration of how advanced temporal control of droplet spacing can be realized and points to the potential of such networks for emerging lab-on-chip applications (e.g., non-electronic based information processing; Hashimoto et al. 2009; Riesco-Chueca and Gan-Calvo 2007). Thus, our results highlight a new route to code and decode signals compared to earlier studies that use drop decision-making events in networks.

Given that ladders with mixed combinations of bypasses can display nonlinear behavior, we ask what degree of nonlinearity can be achieved in ladders. A qualitative indication can be obtained by considering reversibility in ladder networks. Reversibility implies that the original input delay is recovered when the flow is reversed. Ladder networks are reversible because of the absence of decision-making events (Schindler and Ajdari 2008). This reversibility criterion demands that the relationship between input and output delays remain bijective, i.e., there is a one-to-one correspondence between the input and output spacing. In addition, this functional relationship cannot have maxima, minima or saddle points because it has to be strictly monotonic. Thus, we believe reversibility imposes bounds on the degree of nonlinearity that can be achieved with microfluidic ladders.

7 Conclusions

In this paper, we have demonstrated that asymmetric ladder networks give enhanced temporal control of droplet spacing compared to symmetric ladders. We assumed a simple network model to understand asymmetric ladder networks, and the key findings—such as contraction, expansion, synchronization and flipping—were validated using experiments. The effects of finite drop size and waiting times at junctions were neglected in our models. The recent volume-of-fluid modeling of drop transport in symmetric ladder networks has indicated stronger contraction effects than predicted by the simple resistive network model (Song et al. 2012). Therefore, we anticipate that in experimental conditions, the effect of asymmetry in ladder networks would be much higher than that predicted by the model.

A significant finding of our work is that MLNs with mixed bypasses display rich dynamics in drop spacing as well as nonlinear behavior. Such ladder networks in fact also exist in natural systems including leaf venation (Roth-Nebelsick et al. 2001), microvasculature (Skalak et al. 1989; Chau et al. 2011) and neural systems (Hosoya et al. 1991). Interestingly, the nonlinear shape of Fig. 6a resembles that of the widely observed sigmoid function, which is essential for coding/decoding neural signals (Koch and Segev 2000), as it produces an invertible map. Finally, the framework described here can be expanded to explore not only pairs of drops, but also trains of drops to further probe collective hydrodynamics in drop-based microfluidic ladder networks.

Acknowledgments We acknowledge the National Science Foundation for partial financial support (Grant No. CDI-1124814). S.A.V also acknowledges the NSF CAREER Award (Grant No. 1150836) for support.

References

Abbyad P, Dangla R, Alexandrou A, Baroud CN (2011) Rails and anchors: guiding and trapping droplet microreactors in two dimensions. Lab Chip 11:813

Ahn B, Lee K, Lee H, Panchapakesan R, Oh KW (2011) Parallel synchronization of two trains of droplets using a railroad-like channel network. Lab Chip 11:3956

Baret JC, Miller OJ, Taly V, Ryckelynck M, El-Harrak A, Frenz L, Rick C, Samuels ML, Hutchison JB, Agresti JJ, Link DR, Weitz DA, Griffiths AD (2009) Fluorescence-activated droplet sorting (fads): efficient microfluidic cell sorting based on enzymatic activity. Lab Chip 9:1850

Belloul M, Engl W, Colin A, Panizza P, Ajdari A (2009) Competition between local collisions and collective hydrodynamic feedback controls traffic flows in microfluidic networks. Phys Rev Lett 102:194502

Bithi SS, Vanapalli SA (2010) Behavior of a train of droplets in a fluidic network with hydrodynamic traps. Biomicrofluidics 4(1):044110

Bruus H (ed) (2008) Theoretical microfluidics, 1st edn. Oxford University Press, Inc., New York

Chau LT, Rolfe BE, Cooper-White JJ (2011) A microdevice for the creation of patent, three-dimensional endothelial cell-based microcirculatory networks. Biomicrofluidics 5:034115(1)

Cristobal G, Benoit JP, Jaonicot M, Ajdari A (2006) Microfluidic bypass for efficient passive regulation of droplet traffic at a junction. Appl Phys Lett 89:034104

Duffy DC, McDonald JC, Schueller OJA, Whitesides GM (1998) Rapid prototyping of microfluidic systems in poly(dimethylsiloxane). Anal Chem 70(23):4974

Engl W, Roche M, Colin A, Panizza P (2005) Droplet traffic at a simple junction at low capillary numbers. Phys Rev Lett 95:208304

Fuerstman MJ, Garstecki P, Whitesides GM (2007) Coding/decoding and reversibility of droplet trains in microfluidic networks. Science 315:828

Hashimoto M, Feng J, York RL, Ellerbee AK, Morrison G, Thomas III SW, Mahadevan L, Whitesides GM (2009) Infochemistry: encoding information as optical pulses using droplets in a microfluidic device. J Am Chem Soc 131(34):12420

Hong J, Choi M, Edel JB, deMello AJ (2010) Passive self-synchronized two-droplet generation. Lab Chip 10:2702

Hosoya Y, Okado N, Sugiura Y, Kohno K (1991) Coincidence of "ladder-like patterns" in distributions of monoaminergic terminals and sympathetic preganglionic neurons in the rat spinal cord. Exp Brain Res 86:224

Jakiela S, Makulska S, Korczyk PM, Garstecki P (2011) Speed of flow of individual droplets in microfluidic channels as a function

Author's personal copy

of the capillary number, volume of droplets and contrast of viscosities. Lab Chip 11:3603

Koch C, Segev I (2000) The role of single neurons in information processing. Nat Neurosci 3:1171

Labrot V, Schindler M, Guillot P, Colin A, Joanicot M (2009) Extracting the hydrodynamic resistance of droplets from their behavior in microchannel networks. Biomicrofluidics. 3:012804

Lee DH, Lee W, Um E, Park JK (2011) Microbridge structures for uniform interval control of flowing droplets in microfluidic networks. Biomicrofluidics 5(3):034117

Maddala J, Rengaswamy R (2012) A genetic algorithm (ga) based rational approach for design of discrete microfluidic networks. In: Bogle IDL, Fairweather M (eds) 22nd European symposium on computer aided process engineering, computer aided chemical engineering, vol 30. Elsevier, pp 507–511. doi:10.1016/B978-0-444-59519-5.50102-7. http://www.sciencedirect.com/science/article/pii/B9780444595195501027

Maddala J, Srinivasan B, Bithi SS, Vanapalli SA, Rengaswamy R (2012) Design of a model-based feedback controller for active sorting and synchronization of droplets in a microfluidic loop. AIChE J 58(7):2120–2130. doi:10.1016/j.expthermflusci.2010.03.011. http://dx.doi.org/10.1002/aic.12740

Prakash M, Gershenfeld N (2007) Microfluidic bubble logic. Science 315:832

Prakash M, Gershenfeld N (2007) Synchronization in microfluidic circuits. Proceedings of micro TAS

Riesco-Chueca P, Gan-Calvo AM (2007) Microfluidic codecs. Small 3(7):1140

Roth-Nebelsick A, Uhl D, Mosbrugger V, Kerp H (2001) Evolution and function of leaf venation architecture: a review. Ann Bot 87:553

Schindler M, Ajdari A (2008) Droplet traffic microfluidic networks: a simple model for understanding and designing. Phys Rev Lett 100:044501

Sessoms DA, Amon A, Courbin L, Panizza P (2010) Complex dynamics of droplet trafic in a bifurcating microfluidic channel: periodicity, multistability, and selection rules. Phys Rev Lett 105:154501

Skalak R, Özkaya N, Skalak TC (1989) Biofluid mechanics. Ann Rev Fluid Mech 21:167

Song H, Chen DL, Ismagilov RF (2006) Reactions in droplets in microfluidic channels. Angew Chem Int Ed 45(44):7336

Song K, Zhang L, Hu G (2012) Modeling of droplet traffic in interconnected microfluidic ladder devices. Electrophoresis 33(3):411

Theberge AB, Courtois F, Schaerli Y, Fischlechner M, Abell C, Hollfelder F, Huck WTS (2010) Microdroplets in microfluidics: An evolving platform for discoveries in chemistry and biology. Angew Chem Int Ed 49:5846

Vanapalli SA, Banpurkar AG, van den Ende D, Duits MHG, Mugele F (2009) Hydrodynamic resistance of single confined moving drops in rectangular microchannels. Lab Chip 9:982–990